A. DAMIAN et al., Direct Electrochemical Regeneration of NADH on Au, Cu and …, *Chem. Biochem. Eng. Q.* **21** (1) 21–32 (2007)

21

Direct Electrochemical Regeneration of NADH on Au, Cu and Pt-Au Electrodes

A. Damian, Kh. Maloo, and S. Omanovic*
Department of Chemical Engineering, McGill University
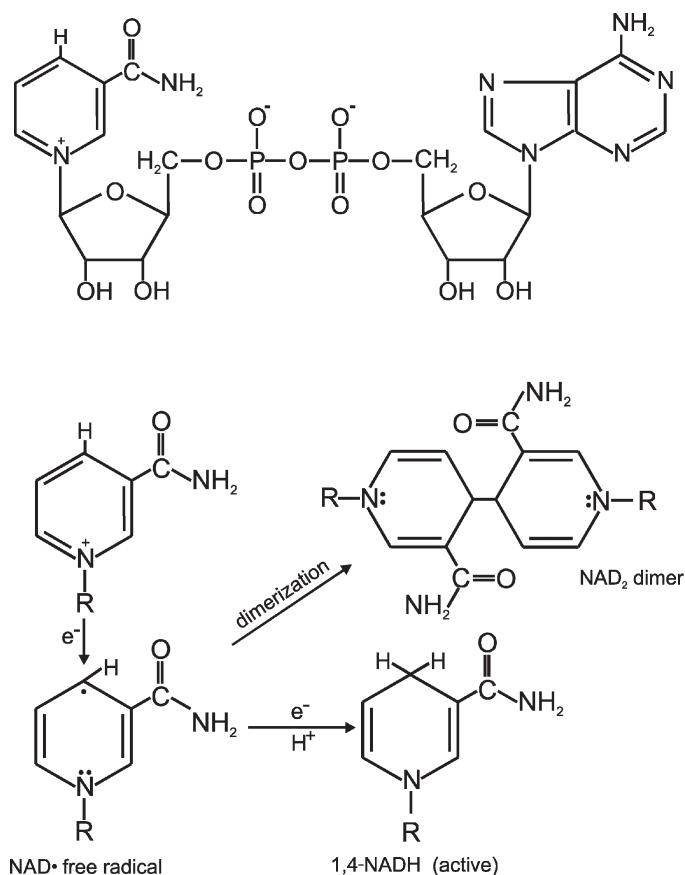Montreal, Quebec, H3A 2B2, Canada

The regeneration of a reduced form of nicotinamide adenine dinucleotide (NADH) in a batch electrochemical reactor employing Au, Cu and Pt-Au electrodes was investigated. The yield of enzymatically active NADH regenerated was found to depend on the electrolysis potential and the electrode material used. At low negative potentials the yield of active NADH regenerated is similar on both Au and Cu, and relatively high (75 % and 71 %, respectively), but the NAD^+ reduction rate and the corresponding conversion degree is low. At high (industrially relevant) negative potentials the NAD^+ reduction rate and the corresponding conversion degree is high, while the yield of active NADH formed on Au is low (28 %) and intermediate on Cu (52 %). In order to increase the yield of enzymatically active NADH formed at high (industrially relevant) potentials, the Au surface was modified with Pt. This resulted in an increase in the yield of active NADH from 29.6 % to 63 %. A reaction mechanism taking into account the influence of Pt is proposed.

Key words:
NADH regeneration, NAD^+ reduction, electrochemical reactor, gold, platinum, copper, modified electrodes

Introduction

About one hundred biochemical reactions catalyzed by redox enzymes (dehydrogenases or oxido-reductases) are dependent on cofactor nicotinamide adenine dinucleotide NAD(H) (Scheme 1). The cofactor plays the role of electron and hydrogen shuttle. In its reduced and enzymatically active form (1,4-NADH), the molecule transfers two electrons and a proton to a substrate in the presence of a suitable enzyme, resulting in the oxidation of NADH to NAD^+. However, the major limitation for its large-scale industrial use is its high cost. Therefore, it would be very beneficial to develop methods that could regenerate NADH *in situ* and allow its catalytic quantities to be used in bioreactors. *Chenault* and *Whitesides*[1], in their review paper on the regeneration of NADH for use in organic synthesis, have classified strategies for NADH regeneration into four general categories: enzymatic, electrochemical, chemical/photochemical, and biological. Taking into account factors influencing the stability and lifetime of NADH in a solution, as well as process considerations that are relevant to the use of NADH in synthesis, they have shown that electrochemistry offers a range of advantages compared to others processes; low-cost, simple monitoring of the reaction progress, and easy product isolation. Hence,

*Author to whom correspondence should be addressed:
Prof. Sasha Omanovic, Department of Chemical Engineering, McGill University, 3610 University Street, Montreal, QC, H3A 2B2, Canada
Phone: (514) 398-4273, Fax: (514) 398-6678,
Email: sasha.omanovic@mcgill.ca

S c h e m e   1 – *Nicotinamide adenine dinucleotide in its oxidized form (NAD+), and its reduction to enzymatically active 1,4 NADH and enzymatically inactive dimer NAD2. R stands for adenosine diphosphoribose.*

the electrochemical reduction of NAD^+ to NADH (*i.e.* NADH regeneration) has attracted considerable scientific attention over the years.

Fundamental aspects of the mechanisms and kinetics of NAD^+ reduction have been investigated using mostly bare (non-modified) high-hydrogen-evolution-overpotential electrodes, such as mercury[2–11] and various carbon materials.[12] It has been shown[3–6] that the reduction of NAD^+ on Hg proceeds by the transfer of one electron to the pyridinium ring, but at significantly high cathodic overpotentials (*ca.* -1.2 V*vs.*SCE at pH 7), followed by fast radical coupling to form an enzymatically inactive dimer NAD_2 (see Scheme 1). The fast dimerization reaction, coupled with the slow second reaction step (electron-transfer and protonation, Scheme 1) is the major reason why the direct reduction of NAD^+ on non-modified electrodes results predominantly in the formation of NAD_2, rather than NADH.[3,7,13] Only by polarizing the Hg electrode further to extreme cathodic overpotentials (*ca.* -1.6 V*vs.*SCE), the formed radical could be partially protonated and further reduced to both 1,4-NADH and 1,6-NADH.[5–7]

Due to the industrial importance of NADH, many attempts have been made to modify electrode surfaces in order to increase the kinetics of the second reaction step (electron transfer and/or protonation, Scheme 1), thus preventing the formation of the dimer and enhancing the stereospecificity of the reduction reaction. Electrochemical systems using chemically-modified[14–20] and enzyme-modified electrodes[21–26] have been proposed. *Baik et al.*[14] have investigated the reduction of NAD^+ using both unmodified and cholesterol-modified gold, gold-amalgam and platinum electrodes. The reduction of NAD^+ on a gold-amalgam unmodified electrode has given only *ca.* 10% enzymatically active NADH, while the yield in active NADH has increased to 50 % when an unmodified platinum electrode has been used. However, when the gold-amalgam electrode has been modified with cholesterol, the yield of active NADH has increased to *ca.* 75 %. Our assumption is that the cholesterol layer attached to the electrode surface served as a physical barrier that prevented dimerization of formed radicals, although the authors have not stated this assumption in the paper. Similarly, *Long* and *Chen*[15] have modified a silver electrode with covalently adsorbed L-histidine, which has resulted in the reduction of NAD^+ to NADH at a yield of *ca.* 82 %. *Shimizu et al.*[16] have immobilized Rh^{3+} ion into a polymeric anion doped-polypyrrole layer formed on the graphite electrode to regenerate NADH. Depending on the anion and polymer used, the yield of enzymatically active NADH has ranged from 26 % to 52 %, while the highest NAD^+ con-version to NADH (both active and inactive) obtained has been *ca.* 50%. *Beley* and *Collin*[17] have also shown that NAD^+ could be reduced to enzymatically active NADH when a reticulated vitreous carbon electrode is covered by a layer of polypyrrole rhodium bis-terpyridine. *Warriner et al.*[18] have modified the surface of a platinum electrode with a poly(3-methylthiophene):poly(phenol red) film, which served as an electron mediator for reduction of NAD^+ to NADH. They have shown that this configuration, which has been developed as a biosensor configuration, is capable of regenerating a certain amount of enzymatically active NADH. Similarly, *Karyakin et al.*[19] have used poly(neutral red)/NAD^+/alcohol-dehydrogenase/Nafion modified glassy carbon electrode in a biosensor configuration to investigate the possibility of active NADH regeneration. They have demonstrated that the detection of acetaldehyde is possible using this electrode, thus showing that the formation of active NADH can be achieved. However, in the latter two papers[18,19] the authors have not reported the yield of the active NADH. Lately, *Vuorilehto et al.*[20] have regenerated active NADH at a very high yield (*ca.* 99 %) using an indirect method with synthesized (pentamethylcyclopentadienyl-2,2'-bipyridine aqua) rhodium (III) as mediator. The mediator was not specifically bound to the 3-dimensional carbon paste cathode but dissolved in the electrolyte together with the nicotinamide cofactor and pumped through the bioreactor.

Due to the problem related to the low selectivity of unmodified and chemically modified electrodes to NADH regeneration, the enzymatically catalyzed (electro)reduction of NAD^+ has also attracted a considerable attention, for both biosensor development and larger-scale applications (*e.g.* bioreactors). *Fry et al.*[21–23] have published a series of papers on the reduction of NAD^+ to NADH on glassy carbon and vitreous carbon electrodes modified by a layer of immobilized methyl viologen and lipoamide dehydrogenase. They have shown that the enzyme catalyzed reduction of NAD^+ on such modified electrodes results in the production of enzymatically active NADH, but the yield of active NADH produced has not been explicitly reported. *Chen et al.*[24] have presented their results on the evaluation of *in situ* methods for the electroenzymatic regeneration of NADH in a packed-bed membrane reactor, and have concluded that the direct electrochemical regeneration of NADH is not feasible in the proposed configuration, but requires the use of methyl viologen and enzyme lipoamide dehydrogenase. They have also concluded that the most efficient method is to immobilize the mediator and enzyme on the electrode using Nafion. No information on the amount of active NADH has been reported in the paper. An important contribu-

tion this field has also been made by *Kim et al.*[25,26] in their papers that discuss the kinetics of the interaction of methyl viologen and diaphorase enzyme for the electrocatalytic reduction of NAD^+ using a gold-amalgam electrode.

However, even if the chemically modified electrodes seem to be an effective approach to prevent the dimer formation and/or enhance the protonation, it has been shown that these previously used modified electrodes lack long-term stability and durability due to the loss of the modification layer under the applied reduction conditions. Similarly, the electro-enzymatic NADH regeneration results in a rather complex electrode system due to difficulties related to immobilization of an enzyme and electron mediator at the electrode surface, loss of the enzyme activity, electron-mediator leakage and also rather slow NADH regeneration rate. Therefore, in order to achieve long-term stability and high yield of enzymatically active NADH, we have designed an 'all-solid' electrode surface by modifying a glassy carbon electrode with a sub-monolayer of ruthenium.[27,28] We have shown that this type of modified electrode can produce a very high yield (*ca.* 96 %) of enzymatically active NADH.

In this paper we are presenting results on the regeneration of enzymatically active NADH in a batch electrochemical reactor using both bare (Au and Cu) and modified (Pt-Au) metallic electrodes. We will show that the yield of active NADH regenerated depends on the electrolysis potential and type of the working electrode used in the reactor. We will also prove our hypothesis that an increase in the yield of active NADH can be achieved by modifying a bare metal electrode that offers high hydrogen evolution overpotential (Au) with a sub-monolayer of a metal that offers low hydrogen evolution overpotential (Pt).

Experimental

The regeneration of NADH from NAD^+ was studied in $c = 0.05$ mol dm^{-3} phosphate buffer solution at pH 7.0 and temperature of 295 K. The buffer was prepared by dissolving monobasic KH_2PO_4 (Sigma, P-5379) in ultra-pure deionized water (resistivity $\rho = 18.2$ MΩcm) and adding 0.10 mol dm^{-3} sodium hydroxide (made from concentrated volumetric solution, ACP Chemical Inc) to adjust pH. To avoid interference (adsorption) of phosphate anions, linear polarization measurements were made in $c = 0.1$ mol dm^{-3} $NaClO_4$ (ACS certified from Fisher), instead of in phosphate buffer. A NAD^+ solution was prepared by dissolving a proper amount of β-NAD^+ (sodium salt, purity 98 %, Sigma N-0632) in $c = 0.05$ mol dm^{-3} phosphate buffer pH 7.0.

A standard three-electrode, two-compartment electrochemical batch reactor was used in all experiments. The counter electrode was a platinum wire of high purity (99.99 %, Johnson-Matthey), which was degreased by refluxing in acetone, sealed in soft glass, electrochemically cleaned by potential cycling in 0.5 mol dm^{-3} sulfuric acid, and stored in 98 % sulfuric acid. During the measurement, the counter electrode was separated from the main reactor compartment by a glass frit. The reference electrode was a commercially available mercury/mercurous sulfate electrode (MSE; +0.400 V *vs.* SCE), but all potentials in this paper are referred to a saturated calomel electrode (SCE). Three different working electrode materials were used in experiments; gold, platinum-modified gold, and copper. The gold working electrode was made of a gold-sputtered glass slide (EMF Corp., glass + 5 nm Ti + 100 nm Au) of $A = 6.1$ cm² geometric surface area. Before each experiment, the slide was first thoroughly cleaned with water and ethanol in an ultrasonic bath, and then electrochemically pretreated (cleaned) in 0.5 mol dm^{-3} perchloric acid by potentiodynamic cycling (40 cycles) between –0.3 and 1.5 V at a potential scan rate of ν = 300 mVs⁻¹. The modification of the gold substrate by platinum was done by the electrodeposition of a Pt sub-monolayer. The sub-monolayer was potentiostatically deposited onto the prepared Au substrate at 0.4 V from $c = 0.1$ mmol dm^{-3} H_2PtCl_6 solution in 0.1 mol dm^{-3} H_2SO_4. The relative amount of platinum was determined by measuring the charge under the hydrogen oxidation/desorption peak in a phosphate buffer solution. The Cu electrode used for NADH regeneration was a plate of $A = 13.8$ cm² geometric surface area. Before each measurement, the copper electrode was prepared by mechanical wet-polishing using #600 and #1500 grit sand papers, then rinsed with deionized water and ethanol, and cleaned in an ultrasonic bath for 5 min.

All the measurements were carried out in an oxygen-free solution, which was achieved by continuous purging of the reactor with argon gas (99.998 % pure). The initial volume of the NAD^+ solution used in all the NADH regeneration measurements was 30 mL. Electrochemical techniques of linear polarization and cyclic voltammetry and chronoamperometry were employed using an Autolab potentiostat/galvanostat PGSTAT 30, handled by the GPES v.4.9 software, while a Varian UV/VIS spectrophotometer was used for the qualitative and quantitative measurements of the electrolysis products and activity assays.

The yield of enzymatically active NADH obtained by electrolysis of NAD^+ was determined using the Sigma Quality Control Test Procedure, EC 1.8.1.4 which was further modified for this purpose

(see Appendix). First, a volume of $V = 0.2$ cm^{-3} of substrate (DL-6,8-thioctic acid amide) and $V = 0.1$ cm^{-3} of EDTA were added into 2.6 mL of produced NADH in the cuvette (3 cm^{-3}). The absorbance of the solution at 340 nm (A_{340}) was monitored (recorded) using a UV-VIS spectrometer, until reaching a steady-state value. Then, the enzyme (lipoamide dehydrogenase) was injected into the cuvette and the absorbance was recorded until reaching a constant value, indicating that the entire active NADH formed during the electrolysis was consumed by the enzymatic reaction. Finally, the yield of active NADH produced by electrolysis was calculated.

Results and discussion

Linear polarization measurements

Linear polarization experiments were first done in order to determine the potential region of NAD$^+$ reduction. Fig. 1 shows the linear polarization curves recorded on polycrystalline gold and copper electrodes in the absence (dashed line) and presence (solid line) of NAD$^+$ in the electrolyte. An increase in current at high negative potentials in the supporting electrolyte (dashed line) is due to the hydrogen evolution reaction, which is more kinetically favorable on the copper electrode. However, when NAD$^+$ is present in the solution (solid line), a significantly higher cathodic current is recorded on both surfaces, as the result of NAD$^+$ reduction. Taking into account that formal potential of the NAD$^+$/NADH couple at the given conditions is $E = -0.485$ V[29], the results in Fig. 1 indicate that the NAD$^+$ reduction reaction is, from the electrochemical point of view, highly irreversible, *i.e.* it occurs at some appreciable rate (high current densities) only at high cathodic overpotentials. Nevertheless, the NAD$^+$ reduction potential region on Au and Cu (Figure 1) is in agreement with that obtained on cholesterol-modified and pure gold-amalgam electrodes[14], mercury electrode,[6] glassy carbon[12,28] and ruthenium-modified glassy carbon (RuGC) electrode,[27,28] and basal pyrolytic graphite electrode.[30] All these data indicate that the NAD$^+$ reduction overpotential is not electrode material dependent, *i.e.* it does not depend on the electrode Fermi level position. In fact, in our recent paper[31] we have shown that the NAD$^+$ reduction potential is dependent on the orientation of the nicotinamide moiety on the electrode surface. Namely, at higher potentials (positive of the formal potential), the nicotinamide moiety is adsorbed on the electrode surface in a vertical-like orientation, which results in an increased electron-transfer tunneling distance, and, thus, inhibited NAD$^+$ reduction. However, by polarizing the electrode surface to negative potentials (negative of the
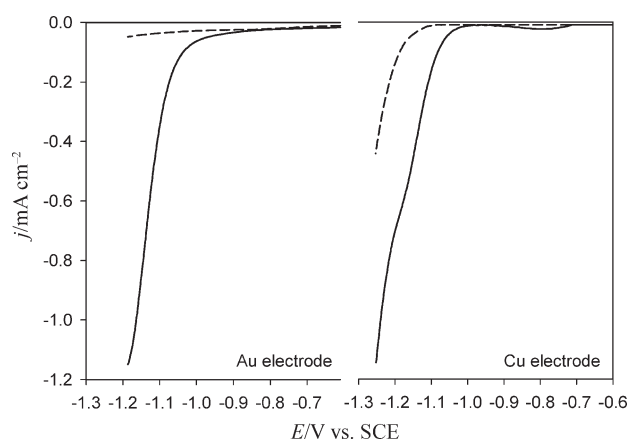

F i g . 1 – *Linear polarization curves of Au and Cu electrodes recorded in 0.1 mol dm^{-3} NaClO$_4$ (dashed line) and 0.1 mol dm^{-3} NaClO$_4$ + 6 mmol dm^{-3} NAD$^+$(solid line). Scan rate, $\nu = 300$ mVs^{-1}.*

formal potential) the nicotinamide moiety tilts towards the electrode surface to a flat orientation, which allows the electron-transfer to occur, and thus the reduction of NAD$^+$. Our polarization modulation infrared reflection absorption spectroscopy[31] and electrochemical impedance spectroscopy[32] measurements confirmed that the NAD$^+$ reduction reaction can be initiated already at –0.5 V and –0.7 V, respectively, but the quantities reduced are negligible. On the other hand, Fig. 1 clearly demonstrates that, to reduce NAD$^+$ at some appreciable rate, which is necessary in order to regenerate NADH for industrial purposes, the polarization of the working electrode to rather high potentials is needed.

Nevertheless, the goal of the project reported in the current paper was not to design an electrode surface that would be capable of reducing NAD$^+$ at lower overpotentials, but to design an electrode surface that would be capable of producing active NADH at a high yield. Therefore, in order to investigate the suitability of bare Au and Cu electrodes for the regeneration of NADH, long-term potentiostatic experiments were done in a batch electrochemical reactor using large-area two-dimensional electrode surfaces. The electrolysis (regeneration) was done at several selected potentials in the potential region of NAD$^+$ reduction, Fig. 1. UV-VIS spectroscopy was used to monitor the reaction progress, and the enzymatic assay was used to determine the yield of active NADH produced.

NADH regeneration on Au and Cu electrodes

UV/VIS absorption spectroscopy measurements: monitoring of NAD$^+$ reduction reaction progress

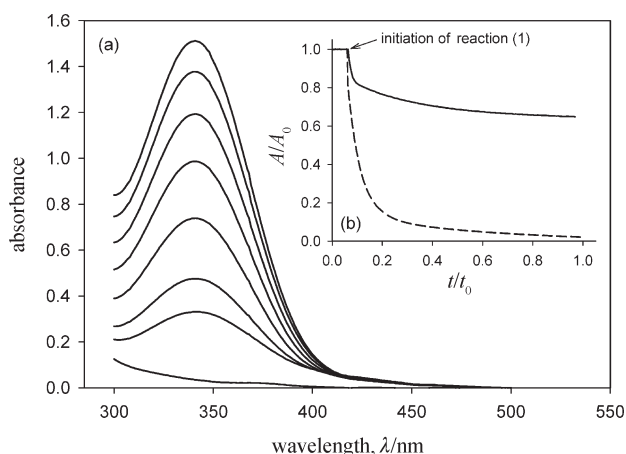Fig. 2a shows the time-dependent UV-VIS response of the Au-based system in the wavelength

F i g . 2 – *(a) Absorption spectra recorded at various times during the electrolysis of a 700 μmol dm⁻³ solution of NAD⁺ in phosphate buffer pH 7.0 on an Au electrode at –1.1 V. The curves shift to higher absorbance values with time: 0, 30, 60, 120, 180, 240, 300 and 360 min. (b) Time dependence of normalized absorbance (A/A₀) of commercial 1,4-NADH (dashed line) and 1,4-NADH produced by electrolysis of a 700 μmol dm⁻³ NAD⁺ solution on an Au electrode at –1.1 V (solid line). A₀ is the absorbance value recorded before reaction (1) was initiated, while A is the absorbance recorded at any time after the initiation of reaction (1).*

region of interest. Before the electrolysis started, *i.e.* in the NADH-free solution, the UV-VIS spectroscopy scan gave only one absorbance peak located at 259 nm (not shown here). This is a well-known peak[7] related to the summation of contributions from the nicotinamide and adenine moiety of NAD⁺ ($\varepsilon_{NAD^+}^{259} = 17800$ dm³ mol⁻¹ cm⁻¹). However, as the electrolysis proceeded, a new peak located at 340 nm appeared, the intensity of which increased with time (Fig. 2a). This peak is related to the selective absorbance of NADH ($\varepsilon_{NADH}^{340} = 6230$ dm³ mol⁻¹ cm⁻¹), but could also be related to the absorbance of dimer NAD₂ ($\varepsilon_{NAD_2}^{340} = 7215$ dm³ mol⁻¹ cm⁻¹)[7]. A very similar response was obtained with the Cu electrode. In Fig. 3 the change in relative absorbance at 340 nm with time for the regeneration of NADH on Au and on Cu electrodes is shown. For both cases, with an increase in time the absorbance increases, indicating the progress of the reaction. At longer times the absorbance approaches a plateau, indicating the completion of NAD⁺ reduction. It appears that the equilibrium is reached faster at lower regeneration potentials, accompanied with relatively low conversion. Since the electrolysis was done at constant potential, the observed two effects are most likely due to a decrease in the electron-transfer driving force (*i.e.* overpotential) with a decrease in [NAD⁺]/[NADH] ratio with time, which is in accordance with the Nernst equation.[32]
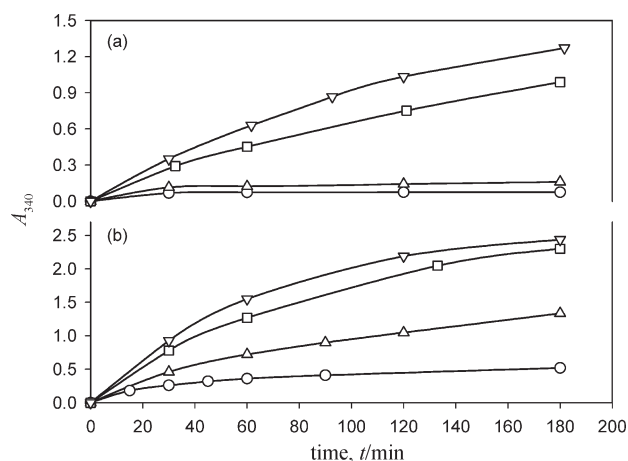

F i g . 3 – *Time dependence of absorbance recorded at 340 nm during the electrolysis of a 700 μmol dm⁻³ solution of NAD⁺ in phosphate buffer pH 7.0 on (a) Au electrode at (O) –0.95, (Δ) –1.00, (□) –1.05, (∇) –1.20 V, and (b) Cu electrode at (O) –0.95, (Δ) –1.00, (□) –1.10, (∇) –1.20 V.*

Absorbance-based initial NAD⁺ reduction reaction rate

Fig. 3 shows that both the reduction rate and the conversion degree increase with an increase in regeneration potential. In order to get preliminary information on the influence of the electrolysis potential on the regeneration reaction rate, the initial regeneration rate, based on the measured absorbance change $(dA/dt)_E$, was determined from the slope of the A_{340} *vs.* time curve at short times at each potential. To eliminate the influence of the electrode surface area, the data were first normalized with respect to the corresponding surface area. The obtained results are presented in Fig. 4. The
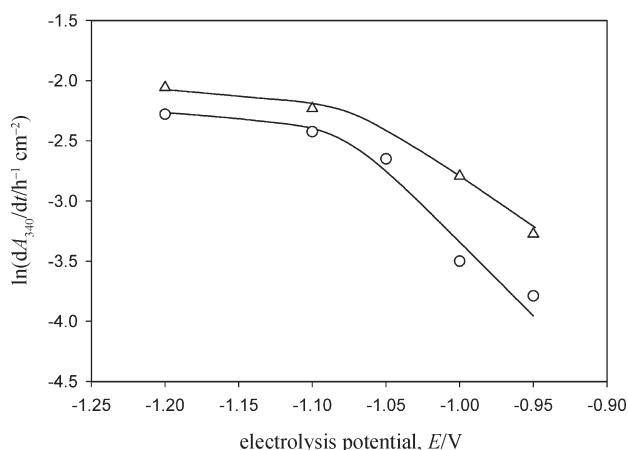

F i g . 4 – *Dependence of the absorbance-based initial NAD⁺ reduction rate on the electrolysis potential calculated from electrolysis of a 700 μmol dm⁻³ solution of NAD⁺ in phosphate buffer pH 7.0 using (O) Au and (Δ) Cu electrode. The values were normalized with respect to the geometric surface area of the electrodes. The lines are included only as a visual aid, and do not represent efforts to model the experimental data.*

figure shows that with an increase in electrolysis overpotential, the initial regeneration rate also increases in an almost linear manner, and then levels off into a plateau at high cathodic overpotentials. Hence, at low overpotentials the NAD$^+$ reduction reaction appears to be electron-transfer controlled, while at high overpotentials mass-transport controls the overall rate of the NAD$^+$ reduction reaction. This is quite in agreement with our linear-polarization kinetic measurements on a gold rotating-disc-electrode[32].

Determination of yield of active NADH

The results in Fig. 3 and 4 demonstrate that with an increase in regeneration potential, both the NAD$^+$ reduction rate and conversion degree increase. However, these results give no information on the yield of active NADH and inactive NADH and NAD$_2$ formed during the electrolysis. To obtain this information, activity assays were done according to the procedure described in the experimental part and Appendix. It should be noted that the original Sigma assay procedure, which was developed to test for the activity of lipoamide dehydrogenase, had to be modified in order to test for the activity of NADH produced by electrolysis. Fig 2b shows the trend of normalized absorbance measured at 340 nm with time for the case of commercially available NADH (98 % active, dashed line) and for NADH produced by electrolysis of 700 μmol dm^{-3} of NAD$^+$ at $V = -1.1$ V using the gold electrode (solid line). Determination of the yield of active NADH produced by electrolysis of NAD$^+$ was based on the following reaction (the detailed experimental procedure is outlined in Appendix):

$$\text{NADH} + \text{DL-lipoamide} \xrightarrow{\text{lipoamide dehydrogenase}}$$

$$\text{NAD}^+ + \text{dihydrolipoamide} \tag{1}$$
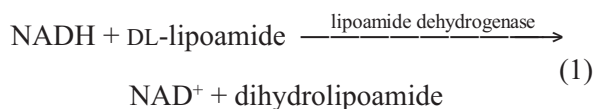
where DL-Lipoamide (substrate) is reduced to dihydrolipoamide in the presence of lipoamide dehydrogenase (enzyme). In order for Reaction (1) to occur, active NADH (cofactor) is required. In order to ensure that all the active NADH produced by the electrochemical regeneration of NAD$^+$ is consumed in reaction (1), the substrate and enzyme were added in excess. It is important to remember that the absorption peak at 340 nm (Figure 2a) is related to the summed response of active and inactive NADH, and the dimer. However, since reaction (1) consumes only the active form of NADH, a decrease in absorbance at 340 nm is then proportional only to the amount of active NADH present in the solution. By setting the absorbance at 340 nm measured before reaction (1) was initiated, A$_o$, as the background (initial) value, and then by monitoring

the decrease in absorbance, A, with time after reaction (1) was initiated, the response presented in Fig 2b was obtained. Then, the yield of active NADH obtained by electrochemical regeneration of NAD$^+$ was calculated as the difference between the initial and final normalized absorbance values:

$$Q_{\text{NADH}} = 1 - \left(\frac{A}{A_0} \right)_{t/t_0 = 1} \tag{2}$$

Fig. 2b shows that the experiment with the commercial NADH (dashed line) confirmed the 98 % activity of the molecule, thus validating the accuracy of the modified assay procedure. On the other hand, the relative absorbance recorded with the NADH produced by electrolysis of NAD$^+$ levels off quickly (Fig 2b, solid line), indicating that only a small amount of the produced NADH is active *i.e.* the main product of the electrolysis is the enzymatically inactive NADH and/or the dimer, NAD$_2$. Using eq. (2) and the result in Fig. 2b it was calculated that only 29.6 % of the converted NAD$^+$ was enzymatically active NADH. The same experiment was done at various potentials using the Au and Cu electrodes, and the results are shown in Fig. 5 as the dependence of percentage of active NADH regenerated (*i.e.* yield) on the electrolysis potential. The results in the figure demonstrate that the yield of active NADH is highly potential dependent. On the Au electrode, the yield of enzymatically active NADH varies from 27.7 % at high overpotentials, up to 75.2 % at low overpotentials, while on the Cu electrode it varies from 51.8 % up to 70.9 %. This behavior is quite consistent with the one expected for organic reactions involving the formation of radicals.[33] With an increase in reduction overpotential the yield of active NADH formed decreases, which is due to an increase in the dimerization rate.
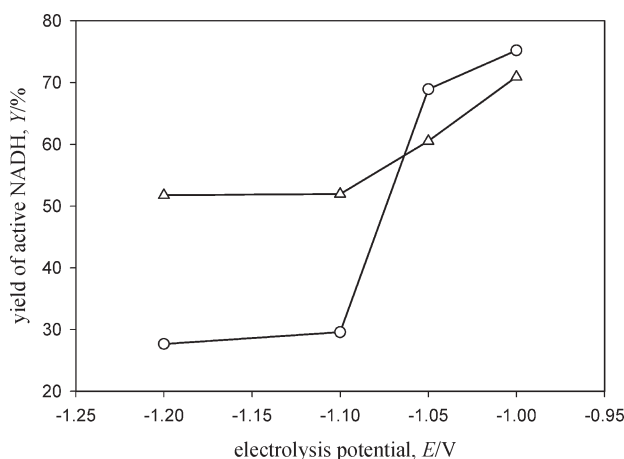

F i g . 5 – *Yield of active 1,4-NADH produced by electrolysis of a 700 μmol dm^{-3} solution of NAD$^+$ in phosphate buffer pH 7.0 at various potentials using (O) Au and (Δ) Cu electrode*

Namely, with an increase in cathodic overpotential, the NAD$^+$ reduction reaction rate also increases, as does the surface amount (coverage) of formed NAD-radicals. Consequently, the probability for two radicals to dimerize also increases. *Yun et al.*[34] have also reported that the amount of enzymatically active NADH regenerated using a platinum electrode and a reactor modified with an anion-charge membrane depended on the electrolysis overpotential. They have also related the lower yield of NADH produced at higher overpotentials to the formation of the dimer. In our case, the highest yield of enzymatically active NADH is found at low overpotentials for both electrodes, and the corresponding yields are very similar, Fig. 5. On the other hand, at high overpotentials, a significantly higher yield of active NADH was obtained on the Cu electrode than on the Au electrode (at –1.2 V it was almost twice higher). This indicates that pure Cu is a better catalyst for NADH regeneration at high (industrially more relevant) overpotentials than Au. Fig. 1 (dashed lines) demonstrates that the hydrogen evolution overpotential is lower on Cu than on Au. Hence, a possible explanation for the better NAD$^+$-reduction electrocatalytic properties of Cu observed at high overpotentials could be that, at these overpotentials a higher amount of adsorbed hydrogen (M-H$_{ads}$) is present on the Cu surface than on the Au surface. Consequently, taking into account the NADH regeneration mechanism (Scheme 1), the higher surface coverage by adsorbed hydrogen facilitates the kinetics of the NADH formation reaction, *i.e.* the second reaction step that involves the hydrogenation/protonation of the NAD-radical.

Nevertheless, the yield of active NADH formed at low overpotentials on both surfaces was surprisingly high compared to the available literature data on the direct regeneration of NADH on other non-modified electrodes[3,7,13]. To the best of our knowledge, besides reference,[34] no other literature reporting a potential dependence of the yield of active NADH formed on other electrodes is available, and thus it is not possible to compare the trend in Fig. 5 to those obtained by other researchers. However, at reported "optimum conditions", only 10 % of active NADH was formed on Au-Hg[14], while a higher yield, 50 %, was obtained on Pt[14] and Hg[7].

Degree of NAD$^+$ conversion

The results in Figure 4 show that the initial NAD$^+$ reduction rate is slightly faster on the Cu electrode than on the Au electrode. However, in order to compare the two electrodes, it would be more convenient to monitor the NAD$^+$ conversion degree for a longer time. For this purpose absorption was first converted into NADH+NAD$_2$ concentration using the Beer-Lambert law, $A = \varepsilon \cdot l \cdot c$, where A corresponds to the measured absorbance, ε to the absorption coefficient for both NADH and NAD$_2$, l to the length of the cuvette (l = 1 cm), and c to the sum of NADH and NAD$_2$ concentration. Then, using the extinction coefficients for NAD$_2$ and NADH listed before in the text and also the ratio between these two species formed during the electrolysis (Fig. 5), the dependence of NAD$^+$ concentration on time was calculated for the Au and Cu electrodes (Pt-Au will be discussed later) and shown in Fig. 6a in terms of the NAD$^+$ conversion. Since the reaction rate depends on both the electrode surface area and solution volume, the time axis was normalized in order to eliminate these two effects. The graph shows that the final conversion of NAD$^+$ was *ca.* 35 % when the Au electrode was used, and 50 % when the Cu electrode was used. Higher conversion on the Cu electrode was also obtained at other potentials. Currently, the exact origin of this difference is unclear, but it might be related to the hydrogen-induced enhancement of diffusion of NAD$^+$ from the solution to the surface. Namely, Fig. 1 shows that Cu is a better hydrogen evolution catalyst than Au. The electrolysis of NAD$^+$ was done in the potential region of hydrogen evolution and, hence, this reaction represents a parallel cathodic reaction. The results in Fig. 4 and our previously published results[32] clearly show that the NAD$^+$ reduction reaction is a mass-transport limited reaction. With electrolysis time, the concentration of NAD$^+$ in the bulk solution decreases, which results in the decreased flux of NAD$^+$ towards the surface,

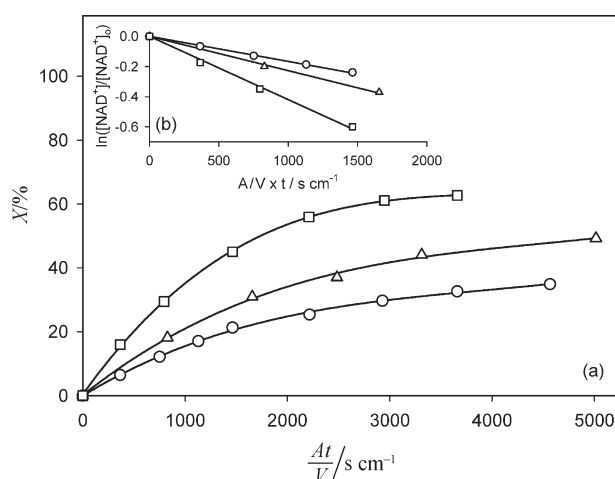F i g . 6 – *(a) Time dependence of NAD$^+$ conversion during the electrolysis of a 700 μmol dm^{-3} solution of NAD$^+$ in phosphate buffer pH 7.0 on (O) Au (at –1.2 V), (Δ) Cu (at –1.2 V) and (□) Pt-Au (at –1.1 V) electrode;*
(b) Dependence of the corresponding normalized NAD$^+$ concentration on electrolysis time. The time axis was normalized with respect to the electrode area and initial volume of the electrolysis solution (30 cm^3).

and thus the decreased NAD⁺ reaction rate (Fig. 6a). However, since the amount of produced hydrogen on the Cu surface is larger than on the Au surface, the produced hydrogen bubbles induce the convection of the solution next to the surface, which ultimately contributes to an increased mass-transport of NAD⁺ towards the surface, and thus the faster NAD⁺ reduction kinetics and the corresponding conversion degree. The conversion degree obtained on another two catalysts that express higher hydrogen evolution activity than pure Au, Pt-Au (circles in Fig. 5, $X = 63$ %) and Ru-glassy carbon (reference 28, $X = 67$ % at –1.2 V) also support this explanation.

Kinetics of NAD⁺ reduction

Our previous results[32] demonstrated that the NAD⁺ reduction reaction performed under both potentiodynamic (linear polarization voltammetry, LPV, and differential pulse voltammetry, DPV, measurements) and potentiostatic conditions (electrochemical impedance spectroscopy, EIS, measurements) is of first order with respect to NAD⁺. In these experiments the reaction rate was measured as the dependence of either current density (LPV/DPV) or charge-transfer resistance (EIS) on the NAD⁺ concentration in the bulk solution. On the other hand, the data in Fig. 6a represents the dependence of NAD⁺ conversion on time, and could also provide information on the kinetics of the NAD⁺ reduction reaction under the applied electrolysis conditions. All the electrolysis experiments were done in a buffer solution pH 7.0 and the measurement of pH before and after the electrolysis confirmed that the pH remained constant during the electrolysis. Hence, the concentration of hydrogen does not change during the electrolysis. Consequently, the reaction rate for the reaction in Scheme 1, r_{NAD+} (mol cm⁻³ s⁻¹), can then be written as[35]:

$$r_{NAD^+} = \frac{d[NAD^+]}{dt} = \frac{1}{V}\frac{dN_{NAD^+}}{dt} = -k'_{NAD^+}[NAD^+]^{\alpha'} \quad (3)$$

where k'_{NAD^+} (cm³ mol⁻¹)$^{\alpha'-1}$ s⁻¹ is the apparent *homogeneous* reaction rate constant with respect to the rate of change in the concentration of [NAD⁺] (mol cm⁻³), and takes into account both the actual reaction kinetics, hydrogen concentration and the mass-transport effect, N_{NAD^+} is the number of moles of NAD⁺ reacted in a unit reactor volume V (cm³), and α' is the partial reaction order with respect to NAD⁺. However, since the investigated reaction is a heterogeneous reaction occurring at the electrode surface, the rate of the reaction depends on the electrode surface area A (cm²). Therefore, it would be more appropriate to express the reaction rate and corresponding coefficient in terms of the rate of change of moles of NAD⁺ per unit surface area of the electrode (mol cm⁻² s⁻¹), rather than per unit volume of the solution (mol cm⁻³ s⁻¹). This basis is more appropriate for heterogeneous (electrochemical) reactions[35]. Hence, this modified rate law for the system investigated can be written as:

$$r_{het,,NAD^+} = \frac{1}{A}\frac{dN_{NAD^+}}{dt} = -k_{NAD^+}[NAD^+]^{\alpha'} \quad (4)$$

where k_{NAD^+} (cm³ mol⁻¹)$^{\alpha'-1}$ cm s⁻¹ is now the apparent *heterogeneous* reaction rate constant. For the first-order reaction, $\alpha' = 1$, the above equation becomes:

$$\ln\frac{(n_{NAD^+})}{(n_{NAD^+})_0} = \ln\frac{[NAD^+]}{[NAD^+]_0} = -k_{NAD^+}\frac{A}{V}t \quad (5)$$

where $(N_{NAD^+})_0$ represents the number of moles of NAD⁺ present in the solution of volume V before the electrolysis, *i.e.* the initial NAD⁺ concentration $[NAD^+]_0$ at time zero. Note that since the volume of electrolyte solution does not change during the electrolysis, the left-hand side of eq. (5) (presented in terms of mol-ratios) can be expressed as concentration ratios. Hence, if the reaction of NAD⁺ reduction is of first order, eq. (5) shows that a plot of $\ln([NAD^+]/[NAD^+]_0)$ versus At/V should give a straight line of slope k_{NAD+}. Indeed, when the electrolysis data presented in Figure 6a are presented in accordance with Eq. (5), a linear relationship is obtained for short electrolysis times, Fig. 6b. At longer electrolysis time, the behavior deviates from linearity, which is both due to the decreased NAD⁺ flux towards the electrode surface and NAD⁺ reduction driving force (overpotential), as already discussed previously in the text. The agreement between the experimental data (symbols) and the model (line) for the first order reaction kinetics, Eq. (5), shown in Fig. 6b is quite in accordance with the results obtained from LPV, DPV and EIS measurements[32]. Now, from the slope of the lines in Fig 6b the apparent heterogeneous reaction rate constant k_{NAD^+} was calculated to be $1.7 \cdot 10^{-4}$ c ms⁻¹ on Au, and $2.3 \cdot 10^{-4}$ cm s⁻¹ on Cu. The corresponding ratio, 1.35, is quite in agreement with the result in Fig. 4, which shows that the initial NAD⁺ reduction reaction rate at –1.2 V is 1.25 times larger on Cu than on Au. Nevertheless, the above k_{NAD^+} values are relatively low, indicating that the overall kinetics of NAD⁺ reduction reaction is slow under the experimental conditions applied. However, it should be noted that the calculated k_{NAD^+} values are apparent values since they are both mass-transport and hydrogen-concentration dependent. Our LPV measurements with a gold rotating-disc-electrode were able to eliminate the influence of mass-trans-

port, and the resulting k_{NAD^+} value calculated at the same overpotential as in Fig. 6b was four orders of magnitude higher. This clearly illustrates the high contribution of mass-transport on the NAD$^+$ reduction rate, as already discussed previously in the text (Fig. 4).

NADH Regeneration on Pt-modified Au Electrodes

Fig. 5 shows that if NADH is regenerated at low potentials (*e.g.* at –1.0 V), a relatively high yield of active NADH can be obtained on pure Au and Cu electrodes. However, the regeneration of NADH at these low potentials is not industrially interesting due to a very slow NAD$^+$ reduction rate and low conversion. On the other hand, the NAD$^+$ conversion is higher at high (industrially relevant) potentials, but the yield of active NADH regenerated is rather low, especially when the Au electrode is used (Fig. 5). Hence, in order to increase the yield of active NADH produced at high potentials, several different electrode modification procedures have been proposed by our laboratory[36]. Namely, the working electrode can be modified by either organic self-assembled-monolayers of alkanethiols (*e.g.* 1-decanethiol) or amino acids (*e.g.* cystine), or by nano-islands of a good hydrogen evolution catalyst (*e.g.* Pt). The purpose of modifying the electrode surface is to physically prevent the dimerization of the two neighboring radicals or/and to increase the rate of the hydrogen addition step (Scheme 1), and in that way to increase the yield of active NADH.

In this paper we have investigated the possibility of modifying the gold surface by platinum nano-islands, Fig. 7. The rationale lies in the NAD$^+$ reduction reaction mechanism presented in Scheme
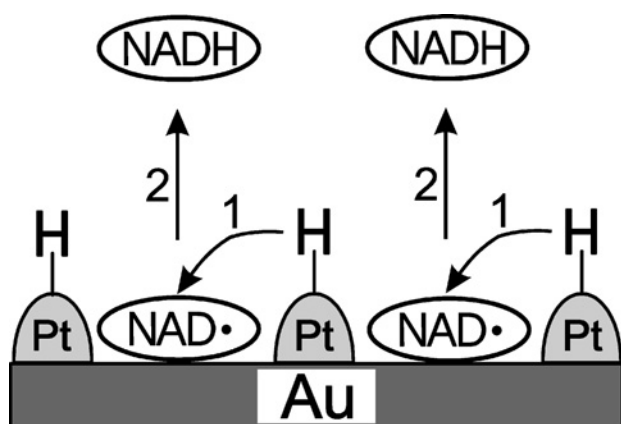

F i g . 7 – *Schematics of the NAD$^+$ reduction reaction mechanism on a Pt-Au electrode. The NAD-radical is formed on the Au part of the surface. This is followed by its hydrogenation with hydrogen adsorbed on the Pt sites (step 1), and then by the second electron transfer to produce NADH (step 2).*

1. As already mentioned, the NAD-radical protonation step is the slow step in the overall reaction mechanism, which on the bare Au electrode polarized at high negative potentials results in the formation of inactive dimer, NAD$_2$ (72 %), rather than active NADH (28 %), as demonstrated in Fig. 5. In order to increase the kinetics of the hydrogen-addition step, it would be preferable to have hydrogen close to the reaction site, *i.e.* adsorbed on the electrode, instead of supplying it from the aqueous solution. In addition, the *hydrogenation* of the NAD-radical, rather than its protonation, would further increase the kinetics of the second step. For this purpose, the electrode surface was modified by a sub-monolayer of Pt, which is a good hydrogen evolution catalyst, Fig. 7. Platinum should ensure that hydrogen, needed in the second reaction step, is already present at the reaction site in the potential region of NAD$^+$ reduction (Fig. 1) as Pt-H$_{ads}$, and the mechanism of hydrogen addition would then be by fast hydrogenation, not rather slow protonation. Also, the Pt sub-monolayer nano-islands would physically prevent the two neighboring radicals from coming into contact and dimerizing. This should ultimately result in an increased yield of active NADH regenerated. This hypothesis is schematically presented in Fig. 7.

As outlined in the experimental section, the modification of the gold substrate was done by the electrodeposition of a sub-monolayer of Pt. The sub-monolayer was deposited potentiostatically onto a prepared Au substrate according to the procedure developed by *Uosaki et al.*[37]. In order to investigate the relationship between the amount of Pt deposited on the Au surface (Pt loading) and the corresponding yield of active NADH produced, long-term potentiostatic electrolysis was carried out at –1.1 V using such modified electrodes. This potential value was chosen since the yield of active NADH formed on pure gold at this potential is low (29.6 %, Fig. 5), and if the above hypothesis had worked, the observed difference would be maximized under these conditions. In addition, at this potential the NAD$^+$ conversion and reduction rate is relatively high, which is relevant for possible industrial applications of the regeneration method.

In order to characterize the electrochemical behavior of the Pt-modified Au electrode, *i.e.* to verify that Pt is deposited on the Au surface, cyclic voltammograms were recorded in a potential domain between –1.2 V and 0.55 V on bare Au and Pt-Au, Fig. 8. The figure demonstrates that there is a significant difference between the behavior of bare Au (dashed line) and Pt-Au (solid line) electrodes. At high cathodic potentials ($E_{cat} < –0.75$ V) the Pt-Au electrode yields a considerably higher hydrogen evolution current density, which is due to the presence
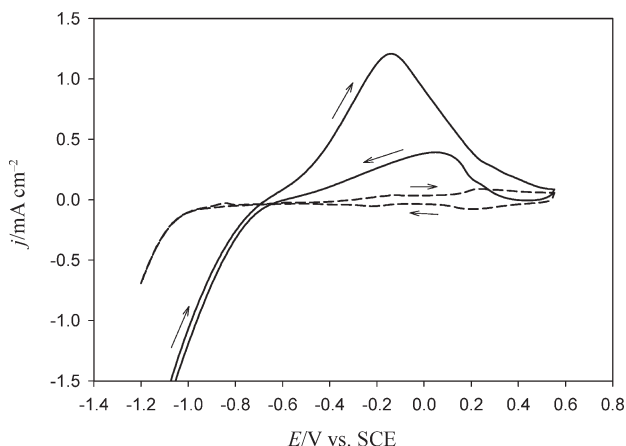
F i g . 8 – *Cyclic voltammograms of a bare Au electrode (dashed line) and a Pt-Au electrode (solid line) recorded in phosphate buffer pH 7.0, scan rate, v = 500 mV s^{-1}.*
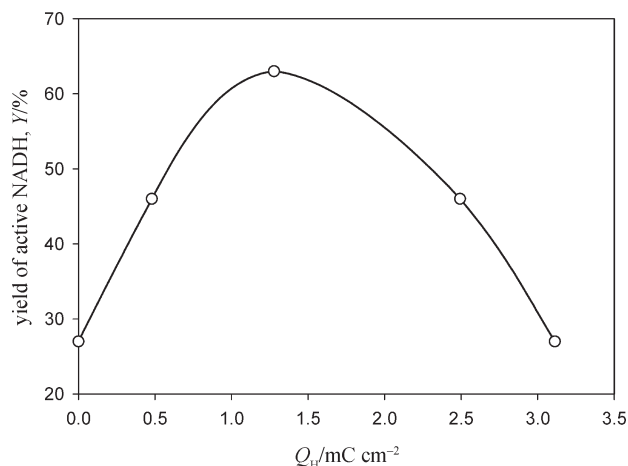

F i g . 9 – *Dependence of the yield of enzymatically active 1,4-NADH produced by electrolysis of a 700 μmol dm^{-3} solution of NAD$^+$ in phosphate buffer pH 7.0 on the apparent amount of platinum deposited on the gold surface. Electrolysis potential, E = –1.1 V.*

of Pt sites on the electrode surface. Moreover, it can be observed that at a fixed current density the corresponding hydrogen evolution overpotential is by ca. 300 mV lower on Pt-Au than on bare Au. Further, at more positive potentials a well-defined broad anodic peak is recorded in the anodic scan. The appearance of the (less-defined and smaller) peak in the returning scan indicates that these two peaks correspond to the oxidation of hydrogen that is both adsorbed on and absorbed in surface Pt sites, but also due to the oxidation of molecular dihydrogen formed at high HER overpotentials ($\eta < $ –0.75 V). All these observations indicate the presence of Pt on the Au surface. Due to the contribution of all three above mentioned effects, it was possible to estimate only an *apparent* amount of platinum on the gold surface by measuring the charge under the anodic peak, but not the true Pt surface area.

Fig. 9 displays the variation of the yield of active NADH produced at –1.1 V with the apparent amount of Pt on the Au surface. The result clearly shows that the yield of active NADH produced depends on the amount of Pt deposited on the Au surface. With an increase in surface coverage by Pt, the yield of active NADH produced also increases, reaching a maximum value of 63 % at $Q = 1.28$ mC cm^{-2}. However, with a further increase in the Pt surface loading (*i.e.* coverage) the yield of active NADH decreases. An origin of this behavior could be related to the competitive effect of the two cathodic reactions, hydrogen evolution and NAD$^+$ reduction, and also to the surface density/distribution of NAD-radical hydrogenation sites, which are the perimeter of Pt islands, *i.e.* the three-interphase Pt/Au/electrolyte region. At low Pt surface coverage, the distance between the adsorbed NAD$^+$ molecule and the (closest) neighboring Pt-H$_{ads}$ site is large. Hence, the formed NAD-radical has to dif-

fuse along the surface towards the Pt-H$_{ads}$ site in order to be hydrogenated. This, in turn, increases the probability for two neighboring NAD-radicals to dimerize and form the enzymatically inactive NAD$_2$. On the other hand, at high Pt surface coverage the predominant reaction is hydrogen evolution. In addition, with an increase in diameter of Pt islands, the number of Au/Pt/electrolyte interphase regions (*i.e.* Pt island perimeters) where the hydrogenation of the produced NAD-radical occurs decreases and thus the probability of the dimerization increases. A balance between these effects observed at the low and high Pt loadings is needed, which seems to be around the Pt surface loading corresponding to charge $Q = 1.5$ mC cm^{-2}, Fig. 9. Nevertheless, these experiments proved our hypothesis that by the modification of the Au surface with Pt results in an increased yield of active NADH produced, from 29.7 % on bare Au to 63 % on the optimized Pt-Au (Fig. 9). These results are also comparable to those obtained by the modification of a glassy carbon electrode with Ru.[27,28]

Another beneficial effect of the modification of the Au surface by Pt is an increased NAD$^+$ conversion degree, Fig. 6a (squares). The graph demonstrates that the NAD$^+$ conversion on Pt-Au is almost twice the conversion on pure Au (63 % *vs.* 35 %, respectively), and is also higher than on pure Cu. The origin of this behavior was already explained previously in the text, and was related to the increased mass-transport by convection induced with produced hydrogen. Fig. 6b (squares) also demonstrates that the NAD$^+$ reduction reaction on Pt-Au is of first order with respect to NAD$^+$. The corresponding apparent heterogeneous reaction rate constant k_{NAD^+} was calculated to be $4.2 \cdot 10^{-4}$ cm s^{-1} at –1.1 V, which is

3.8 times higher than the value obtained on pure Au at the same potential. This clearly shows that the modification of the Au surface also results in increased NAD$^+$ reduction kinetics. Since the k_{NAD^+} is an apparent value that takes into account mass-transport effects, its increase going from Au → Cu → Pt-Au could also be related to the increase in NAD$^+$ flux towards the electrode surface as a consequence of enhanced mass-transport by hydrogen.

Conclusions

The regeneration of NADH in a batch electrochemical reactor was investigated in a phosphate buffer solution pH 7.0. Au, Cu and Pt-Au were used as regeneration (working) electrodes. It was shown that the yield of active NADH produced on the Au and Cu electrodes depends on the electrolysis potential and the electrode material. At low negative potentials the NAD$^+$ reduction rate and the corresponding conversion degree is low, while the yield of active NADH produced is relatively high. On the other hand, at high negative potentials the NAD$^+$ reduction rate and the corresponding conversion degree is high, but the yield of active NADH produced is low, especially on Au. The latter was explained on the basis of high surface concentration of NAD-radicals formed at high potentials, which in turn increases the probability for their dimerization to produce the enzymatically inactive NAD$_2$.

The hypothesis that an increased yield of active NADH can be obtained by modifying the Au surface with Pt was proven. At –1.1 V the yield of active NADH formed increased from 29.6 % on bare Au to 63 % on Pt-Au. This was explained on the basis of both the enhanced kinetics of the second reaction step (hydrogenation of the NAD-radical) and physical prevention (minimization) of the dimerization of the neighboring NAD-radicals. It was also shown that by modifying the Au surface with Pt an increase in the NAD$^+$ conversion degree and NAD$^+$ reduction kinetics can be achieved.
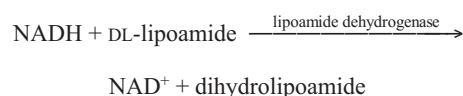
The NAD$^+$ reduction reaction was determined to be of first order with respect to NAD$^+$ on all three electrode surfaces. The corresponding apparent heterogeneous reaction rate constants are rather low, which is due to the slow mass-transport of electroactive species from the solution to the electrode surface.

Appendix: Enzymatic Assay

PRINCIPLE:

$$\text{NADH} + \text{DL-lipoamide} \xrightarrow{\text{lipoamide dehydrogenase}}$$

$$\text{NAD}^+ + \text{dihydrolipoamide}$$

Abbreviations used:

NADH = nicotinamide adenine dinucleotide, reduced form

NAD$^+$ = nicotinamide adenine dinucleotide, oxidized form

DL-Lipoamide = DL-6,8-thioctic acid amide

Dihydrolipoamide = DL-6,8-dihydrothioctic acid amide

CONDITIONS:

T = 25°C, pH 7, $A_{340\ nm}$, light path b = 1 cm

METHOD:

UV-Vis spectrometer

REAGENTS:

A. 100 mmol dm^{-3} phosphate buffer, pH 7 at 25°C

(Prepare 100 cm^3 in deonized water using potassium phosphate, monobasic, anhydrous, Sigma P-5379. Adjust to pH 7 with 1 mol dm^{-3} NaOH).

B. 28 mmol dm^{-3} DL-6,8-thioctic acid amide

(Prepare by dissolving 57.4 mg of DL-6,8-thioctic acid amide, Sigma T-5875, in 6 cm^3 ethanol (nondenatured). Dilute this solution with 4 cm^{-3} reagent A. Prepare fresh).

C. 300 mmol dm^{-3} ethylenediaminetetraacetic acid (EDTA) with φ = 2.0 % Albumin solution, pH 7.

(Prepare 10 cm^3 in deionized water using EDTA, Sigma ED4S and albumin bovine, Sigma A-0281. Adjust to pH 7 with 5 mol dm^{-3} HCl).

D. Nicotinamide adenine dinucleotide, reduced form (NADH) produced by electrolysis of a 700 μmol dm^{-3} solution of NAD$^+$ in phosphate buffer pH 7.0.

E. Lipoamide Dehydrogenase Enzyme Solution

(Immediately before use, prepare a 10 cm^{-3} solution containing 0.6 unit cm^{-3} of lipoamide dehydrogenase, Sigma L-2002 in cold reagent A).

PROCEDURE:

Pipette (in cm^3) the following reagents into suitable cuvettes:

Reagent	Ref 1	Ref 2	Test
A (buffer)	2.6	2.6	–
B (DL-Thio)	0.2	0.2	0.2
C (EDTA)	0.1	0.1	0.1
D (NADH)	–	–	2.6
E (enzyme)	–	–	0.1

First, zero the absorbance at 340 nm with Ref 1 and Ref 2, and then remove Ref. 2 and replace it with Test. Record the change in absorbance at 340 nm with time, until it becomes constant. Then add reagent E and record the absorbance with time until reaching a constant value.

List of symbols

A	–	absorbance
A_s	–	surface area, cm^2
a	–	activity
c	–	concentration, mol dm^{-3}
E	–	potential, V
j	–	current density, mA cm^{-2}
k', k	–	reaction rate coefficient, cm^3 mol^{-1} s^{-1}
l	–	length, m
n	–	amount of substance, mol
Q	–	charge density, C cm^{-2}
R	–	resistance, Ω
r	–	reaction rate, mol cm^{-3} s^{-1}, mol cm^{-2} s^{-1}
T	–	temperature, $^{\circ}$C
t	–	time, h, min
V	–	volume, cm^3
X	–	conversion, %
Y	–	yield, %
ε	–	absorbance coefficient, dm^3 mol^{-1} cm^{-1}
ρ	–	resistivity, Ωm
η	–	overpotential, V

Literature

1. *Chenault, H. K., Whitesides, G. M.,* Appl. Biochem. Biotech. **14** (1987) 147.
2. *Burnett, J. N., Underwood, A. L.,* Biochemistry **4** (1965) 2060.
3. *Schmakel, C. O., Santhanam, K. S. V., Elving, P. J.,* J. Am. Chem. Soc. **97** (1975) 5083.
4. *Bresnahan, W. T., Elving, P. J.,* J. Am. Chem. Soc. **103** (1981) 2379.
5. *Elving, P. J., Bresnahan, W. T., Moiroux, J., Samec, Z.,* Bioelectrochem. Bioenerg. **9** (1982) 365.
6. *Moiroux, J., Deycard, S., Malinski, T.,* J. Electroanal. Chem. **194** (1985) 99.
7. *Jaegfeldt, H.,* Bioelectrochem. Bioenerg. **8** (1981) 355.
8. *Jensen, M. A., Bresnahan, W. T., Elving, P. J.,* Bioelectrochem. Bioenerg. **11** (1983) 299.
9. *Schmakel, C. O., Jensen, M. A., Elving, P. J.,* Bioelectrochem. Bioenerg. **5** (1978) 625.
10. *Bresnahan, W. T., Moiroux, J., Samec, Z., Elving, P. J.,* Bioelectrochem. Bioenerg. **7** (1980) 125.
11. *Studnickova, M., Paulova-Klukanova, H., Turanek, J., Kovar, J.,* J. Electroanal. Chem. **252** (1988) 383.
12. *Moiroux, J., Elving, P. J.,* J. Electroanal. Chem. **102** (1979) 93.
13. *Takamura, K., Mori, A., Kusu, F.,* Bioelectrochem. Bioenerg. **8** (1981) 229.
14. *Baik, S. H., Kang, C., Jeon, I. C., Yun, S. E.,* Biotech. Techniques **13** (1999) 1.
15. *Long, Y.-T., Chen, H.-Y.,* J. Electroanal. Chem. **440** (1997) 239.
16. *Shimizu, Y., Kitani, A., Ito, S., Sasaki, K.,* Denki Kagaku **61** (1993) 872.
17. *Beley, M., Collin, J.-P.,* J. Molec. Cat. **79** (1993) 133.
18. *Warriner, K., Higson, S., Vadgama, P.,* Mat. Sci. Eng. C **5** (1997) 91.
19. *Karyakin, A. A., Bobrova, O. A., Karyakina, E. E.,* J. Electroanal. Chem. **399** (1995) 179.
20. *Vuorilehto, K., Lütz, S., Wandrey, C.,* Bioelectrochem. **65** (2004) 1.
21. *Fry, A. J., Sobolov, S. B., Leonida, M. D., Voivodov, K. I.,* Tetrahedron Lett. **35** (1994) 5607.
22. *Voivodov, K. I., Sobolov, S. B., Leonida, M. D., Fry, A. J.,* Bioorg. Med. Chem. Lett. **5** (1995) 681.
23. *Sobolov, S. B., Leonida, M. D., Bartoszko-Malik, A., Voivodov, K. I., McKinney, F., Kim, J., Fry, A. J.,* J. Org. Chem. **61** (1996) 2125.
24. *Chen, X., Fenton, J. M., Fisher, R. J., Peattie, R. A.,* J. Electrochem. Soc. **151** (2004) E56.
25. *Kim, S., Yun, S.-E., Kang, C.,* Electrochem. Comm. **1** (1999) 151.
26. *Kim, S., Yun, S.-E., Kang, C.,* J. Electroanal. Chem. **465** (1999) 153.
27. *Man, F., Omanovic, S.,* J. Electroanal. Chem. **568** (2004) 301.
28. *Azem, A., Man, F., Omanovic, S.,* J. Mol. Catal. A: Chem. **219** (2004) 283.
29. *Clark, W. M.,* Oxidation and Reduction Potentials of Organic Systems, Williams & Wilkins, Baltimore, 1960.
30. *Nakamura, Y., Suye, S.-I., Kira, J.-I., Tera, H., Tabata, I., Senda, M.,* Biochem. Biophys. Acta **1289** (1996) 221.
31. *Damian, A., Omanovic, S.,* Langmuir, in review
32. *Damian, A., Omanovic, S.,* J.Molec.Catal.A: Chemical, **253** (2006) 222.
33. *Hamann, C. H., Hamnett, A., Vielstich, W.,* Electrochemistry, Wiley-VCH, Germany, 1998.
34. *Yun, S. E., Taya, M., Tone, S.,* Biotechnol. Lett. **16** (1994) 1053.
35. *Levenspiel, O.,* Chemical Reaction Engineering, 3rd Ed., Willey, 1999.
36. *Omanovic, S., Damian, A., Azem, A., Man, F.,* 1st ECHEM Meeting, Venezia, Italy, 2005.
37. *Uosaki, K., Ye, S., Naohara, H., Oda, Y., Haba, T., Kondo, T.,* J. Phys. Chem. B, **101** (1997) 7566.